MOLECULAR IMAGING AND BIOLOGY

Mol Imaging Biol (2019) 21:1026–1033
DOI: 10.1007/s11307-019-01343-4

Published Online: 14 March 2019

WMIS World Molecular Imaging Society

Check for updates

BRIEF ARTICLE

Fluorescent Polymer Dots for Tracking $SKOV_3$ Cells in Living Mice with Probe-Based Confocal Laser Endomicroscopy

Yufan Zhang,[1] Yao Li,[1] Yixiao Guo,[1] Yidian Yang,[1,2] Shiyi Tang,[1] Liqin Xiong[1]

[1]*Shanghai Med-X Engineering Center for Medical Equipment and Technology, School of Biomedical Engineering, Shanghai Jiao Tong University, Shanghai, 200030, People's Republic of China*

[2]*The Key Laboratory of Resource Chemistry of Ministry of Education, Shanghai Key Laboratory of Rare Earth Functional Materials, and Shanghai Municipal Education Committee Key Laboratory of Molecular Imaging Probes and Sensors, Shanghai Normal University, Shanghai, 200234, People's Republic of China*

Abstract

Purpose: Probe-based confocal laser endomicroscopy (pCLE) is a novel technique allowing real-time and high-resolution imaging *in vivo*. It provides microscopic images and increases the penetration depth of tissues compared with conventional white light endoscopy. The aim of the present study was to track ovarian cancer cells in organs by fluorescent polymer dots based on pCLE.

Procedures: $SKOV_3$-mCherry cells were incubated with polymer dots for 24 h in a serum-free culture medium. Labeled cells were administrated to nude mice *via* intravenous, intraperitoneal, and lymph node injection. The fluorescent signals of labeled cells in organs were observed by pCLE. Furthermore, the results were confirmed by frozen section analysis.

Results: pCLE displayed fluorescence signals of labeled cells in the vessels of organs. Besides, the accumulations of labeled cells visualized in detoxification organs like the spleen and kidney were increased with time.

Conclusions: In this article, we present a real-time and convenient method for tracking $SKOV_3$-mCherry in living mice by combined fluorescent polymer dots with pCLE.

Key words: Polymer dots, Fluorescence imaging, pCLE, Tracking, Ovarian cancer

Introduction

Fluorescence imaging has emerged as a powerful modality in biological studies because it offers high signal-to-noise ratios and splendid spatial resolution [1–3], and has proven to be a useful tool for clinical applications [4]. Conjugated polymer dots (Pdots), as an attractive fluorescence probe, provide excellent fluorescence intensity, remarkable photostability and biocompatibility, superior sensitivity, and low toxicity [5–10]. Recently, Pdots have been applied *in vivo* applications including cancer diagnosis and imaging, fluorescence-guided surgery, lymph node mapping, and ultrafast hemodynamic [5, 7, 11–13].

Ovarian cancer leads the significant female health problem in the world and ranks the high mortality rate among all the gynecological malignancies. The early stages are asymptomatic [14–20]. Chan and co-workers synthesized folic acid–functionalized Pdots (FA-Pdots) for *in vivo* targeting and long-term monitoring of ovarian cancers by fluorescence imaging. $SKOV_3$ cells incubated with 1 ml FA-Pdots (15 nM) for 16 h were

Electronic supplementary material The online version of this article (https://doi.org/10.1007/s11307-019-01343-4) contains supplementary material, which is available to authorized users.

Correspondence to: Liqin Xiong; *e-mail:* xiongliqin@sjtu.edu.cn

implanted subcutaneously in nude mice. The fluorescence of the tumor retained 32 % even after 36 days post-injection [21].

Confocal laser endomicroscopy is a new and small field of clinical imaging with a flexible endoscopy which allows high magnification and excellent resolution based on fluorescence imaging. It provides a microscopic approach to study the tissue at cellular and extracellular level *in vivo*. Until now, the technology has affected several strategies of clinical care [22–27]. In this article, we applied probe-based confocal laser endomicroscopy (pCLE) to track ovarian cancer cells labeled with fluorescent polymer dots [28]. Pictures and videos were recorded of five organs including the spleen, kidney, liver, heart, and lung at different imaging times. These data are expected to provide insights into the further applications of pCLE and monitor pathological processes *in vivo*.

Materials and Methods

Poly(9,9-dioctylfluorene-*alt*-benzothiadiazole) (PFBT, average M_n 10 to 20 k) was purchased from Sigma-Aldrich, Inc. Polystyrene (PS) graft ethylene oxide functionalized with PS and carboxylic end group (PS-PEG-COOH) and amino-terminated poly(methyl methacrylate) (MMA-NH_2) were purchased from Polymer Source Inc. Folate Cap PE (PE-FA) was purchased from AVanti, Polar Lipids, Inc. Unless otherwise stated, all chemicals and solvents were of analytical grade and used without further purification.

A reprecipitation method was used to synthesize the functional polymer dots and has been reported in our previous articles [11, 29, 30]. All the raw materials were dissolved in tetrahydrofuran (THF) as 1 mg/ml, respectively. The first step of typical procedures was to add PFBT, PS-PEG-COOH, MMA-NH_2, and PE-FA into 2 ml THF in a fixed ratio. After 5 min of ultrasonication in the water bath, the mixture was quickly dispersed into 10 ml Milli-Q water under vigorous sonication using an ultrasonic cell crusher for 1 min (10 % power). The excess THF was evaporated at 50 °C under the protection of nitrogen (Hannuo Instrument, China). Finally, the solution was filtered with a 0.22 μm of polyvinylidene fluoride membrane. For further application, the suspension of polymer dots was concentrated to different concentrations through a centrifugal filtration device (Amicon Ultra-15 Centrifugal Filter with a molecular weight cutoff of 100 kDa).

Characterization of the Polymer Dots

Morphologies of polymer dots were captured by a HITACHI JEM-2100F transmission electron microscopy (TEM) operated at 120 kV (HITACHI, Japan). The hydrodynamic size and zeta potential of the polymer dots were measured with a Malvern Zetasizer Nano ZSP instrument (Malvern, UK) (DLS). UV–vis absorption spectrum was measured *via* a Shimadzu UV-2550 ultraviolet–vis spectrometer (Shimadzu, China). Fluorescence emission spectrum was collected using a HITACHI F-2700 fluorescence spectrophotometer. The absolute fluorescence quantum yield (QY) was measured by a Hamamatsu UV–NIR absolute PL QY spectrometer (Hamamatsu, Japan) using an integrating sphere with 450-nm excitation for polymer dots from a xenon lamp. In the physical stability test, polymer dots were dispersed in phosphate-buffered saline (PBS, 1×) and McCoy's 5A medium containing 10 % FBS as the same ratio at 37 °C, respectively. Then, the particle size variance was measured by DLS, and the fluorescence spectra were collected to detect the fluorescence stability on an ELISA molecular system (SpectraMax i3x) [11, 31].

Cell Culture and Flow Cytometry Assay

$SKOV_3$ cells, established from a human ovarian adenocarcinoma, were obtained from the Shanghai Institute of Cell Biology of the Chinese Academy of Sciences (Shanghai, China). $SKOV_3$-mCherry cells [20] were kindly provided by Prof. Yu Kang of Shanghai Medical School of Fudan University (Shanghai, China). The cells were grown in McCoy's 5A medium with 10 % FBS and 1 % penicillin/streptomycin. All the culture dishes were cultured in the incubator containing 5 % CO_2 at 37 °C.

$SKOV_3$-mCherry was seeded in a six-well plate (2.4×10^5 cells per well). Then, 5.4 μg of polymer dots was added into every well for 24 h without serum. After 1000 rpm of centrifugation for 4 min, cells of every well were resuspended into 200 μl phosphate-buffered saline (PBS, 1×). Half of the solution was added into 400 μl PBS and analyzed *via* a Becton Dickinson FACSAria II flow cytometry (Becton Dickinson, USA). The rest was cultured in a new six-well plate for the next generation. The fluorescence intensity plot was acquired using the BD FACSAria II software.

Confocal Laser Scanning Microscopy Imaging

In the log growth phase, approximately 3×10^4 $SKOV_3$-mCherry was seeded in a glass-bottom dish and incubated with ~5 μg of polymer dots without serum. After 24-h incubation, the dishes were washed twice with PBS. In the cell staining assay, cells were fixed with 4 % paraformaldehyde (PFA) for 15 min and stained with DAPI solution for 10 min. Cells were observed using a confocal laser scanning microscopy (CLSM) instrument (Leica, Germany). Channel settings were as follows: PFBT (excitation 458 nm, emission 530–600 nm), 4′,6-diamidino-2-phenylindole (DAPI; excitation 405 nm, emission 425–520 nm), and mCherry (excitation 561 nm, emission 600–650 nm).

Fluorescence Intensity Analysis of Polymer Dots and mCherry in Fluorescence Imaging

The 100 μl PBS of 2.5×10^5 $SKOV_3$-mCherry cells was added into each of four wells in an enzyme label plate. Comparatively, 100 μl of polymer dots (~6 μg) was

added in the same way. ROI of every well was analyzed using an IVIS Lumina K imaging system (PerkinElmer, USA).

pCLE Imaging of SKOV$_3$-mCherry in Organs of Living BALB/c Nude Mice

Experiments were conducted based on a Cellvizio Dual Band system (Mauna Kea Technologies, France). A ProFlex S1500 scanning probe was used in this system (diameter = 1.5 mm, spatial resolution = 3.3 µm, $\lambda_{excitation}$ = 488 nm, $\lambda_{detection}$ = 505–700 nm). Each nude mouse was anesthetized with 200 µl PBS solution of pentobarbital sodium (1 %) by intraperitoneal (i.p.) injection. Then, 2×10^6 SKOV$_3$-mCherry incubated with 50 µg polymer dots were syringed into mice by intravenous (i.v.) injection, i.p. injection, and inguinal lymph node injection, respectively. Real-time video sequences were recorded at 12 frames/s. The probe contacted five organs including the spleen, kidney, liver, heart, and lung directly and perpendicularly [23, 32]. pCLE video sequences and images were processed offline using the matching software (IC viewer, Mauna Kea Technologies, France).

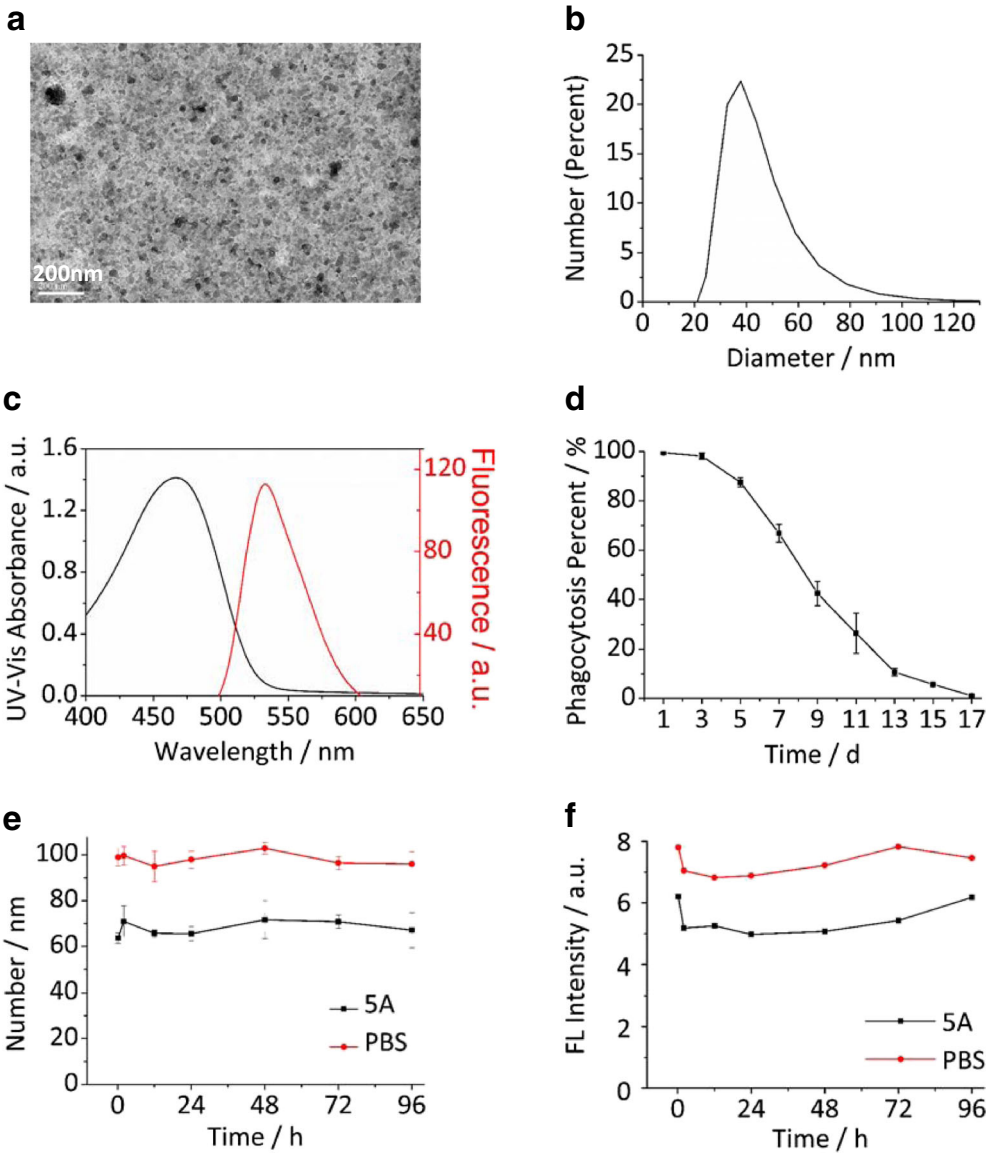

Fig. 1. Characterization of PNCP. **a** TEM image of PNCP. The scale bar is 200 nm. **b** Hydrodynamic diameter of PNCP. **c** UV–vis absorbance and fluorescence spectra of PNCP. **d** Flow cytometry plot of SKOV$_3$-mCherry cells. After incubated with PNCP, SKOV$_3$-mCherry was analyzed for the fluorescence intensity of polymer dots by a flow cytometry at different time points. **e** Particle size variance of PNCP after treatment with PBS or 5A medium containing 10 % FBS for 96 h at 37 °C. **f** Fluorescence stability of PNCP in PBS or 5A medium containing 10 % FBS for 96 h at 37 °C.

Histology Analysis of Organs

Organs were fixed with 4 % PFA. Eight-micrometer-thick frozen sections were obtained using a cryo-microtome (Leica CM1950) and observed by CLSM. The channel was set for PFBT (excitation 458 nm, emission 530–600 nm).

Results

Synthesis and Characterization of Polymer Dots

Polymer dots with PFBT as the matrix were used because of their generally low or absent toxicity, high fluorescence, and long-term stability. PE-FA was employed as a tumor-targeting ligand because the receptor alpha is overexpressed on the surface of epithelial ovarian tumors [33–35]. PS-PEG-COOH and MMA-NH_2 were coated polymer dots as a biocompatible shell to improve the behavior of pharmacokinetics *in vivo*. PFBT polymer dots modified with PE-FA, MMA-NH_2, and PS-PEG-COOH (PNCP) were used for tracking tumor cells *in vitro* and *in vivo*. The synthesis process was shown in Suppl. Scheme 1 (see Electronic Supplementary Material).

The morphology of PNCP was characterized by TEM. As shown in Fig. 1a, they were found to have a spherical shape with an average diameter of 32 nm. The size of PNCP was uniform with a hydrodynamic diameter of 42 ± 4 nm in Fig. 1b. Mean polydispersity index (PDI) is 0.152 and the zeta potential is -34.5 ± 2 mV. Results showed that PNCP had the good dispersity and colloidal stability in water. The differences between TEM data and hydrodynamic diameter data were due to hydration corona formed by the PS-PEG-COOH or MMA-NH_2 polymer chains [11]. The absorption and emission spectra of PNCP in water were shown in Fig. 1c. The peak of absorption was at 467 nm, and the emission spectrum was centered at 535 nm. The absolute quantum

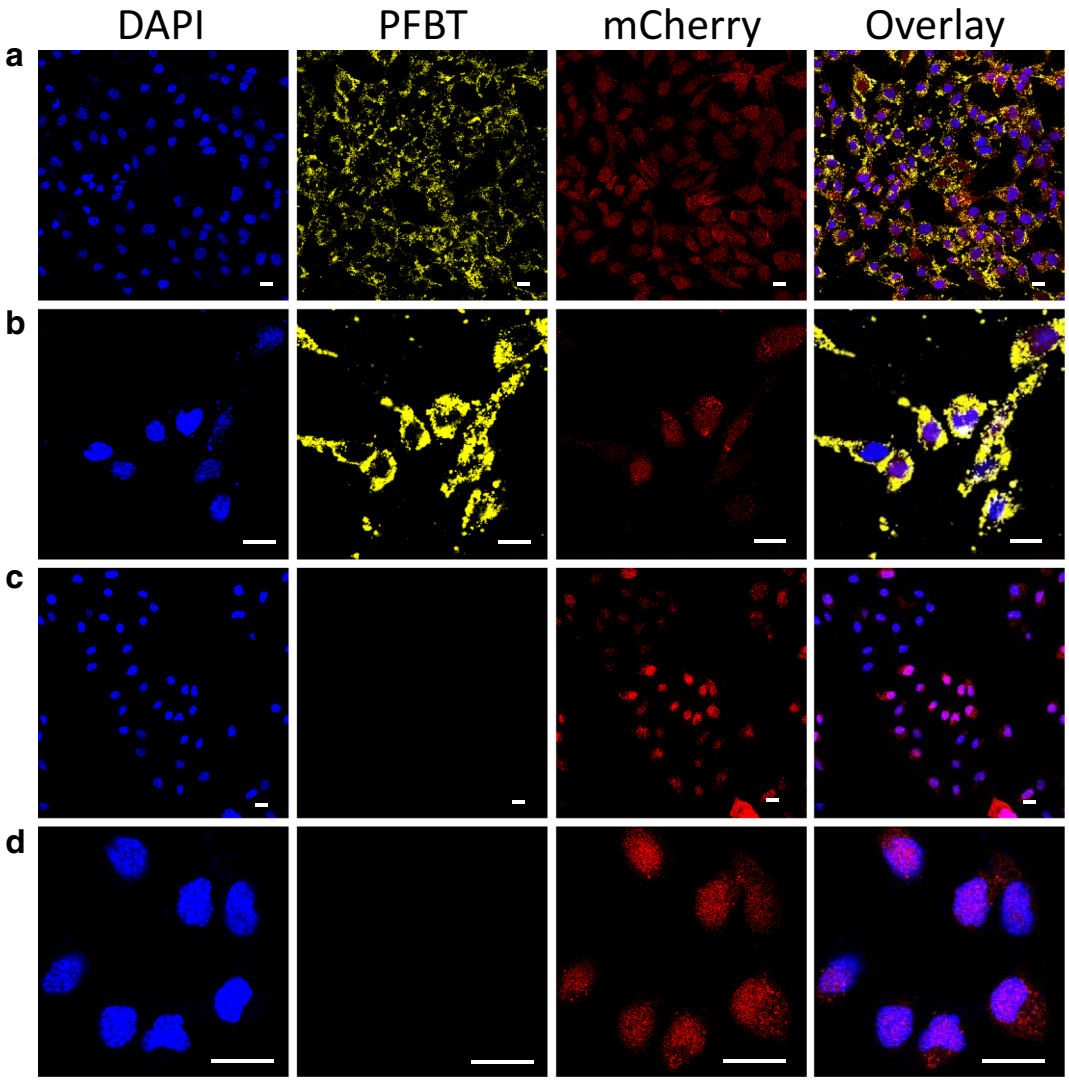

Fig. 2. CLSM imaging of $SKOV_3$-mCherry cells. The scale bar is 20 μm. **a** CLSM imaging of $SKOV_3$-mCherry after 24-h incubation with PNCP. **b** Magnification of panel **a**. **c** CLSM imaging of $SKOV_3$-mCherry. **d** Magnification of panel **c**.

yield (QY) test showed that the value of PNCP was approximately 0.1. In the physical stability test (Fig. 1e), the diameters of PNCP showed no obvious change during 96 h. Besides, the fluorescence intensity showed a slight decrease after 2 h as shown in Fig. 1f. The value of PNCP treated with 5A medium after 96 h maintained approximately 90 % of their original intensities. Comparatively, the value of PNCP treated with PBS increased slightly from 24 to 96 h. These data suggested that these polymer dots have good physical stability.

Flow Cytometry Assay and CLSM Imaging

The fluorescence intensity of PNCP in $SKOV_3$-mCherry was accessed by a flow cytometry. Fig. 1d showed phagocytosis percent of PNCP in $SKOV_3$-mCherry reached 99.5 % ± 0.2 % after 24 h, and PNCP still existed in cells after 15 days. The original charts were displayed in Suppl. Fig. 1 (see Electronic Supplementary Material (ESM)), showing that the peaks of experimental groups were gradually close to the blank group with days increasing. The value was close to zero 17 days later.

In CLSM imaging, PNCP existed in the cytoplasm region while mCherry existed in whole cell (Fig. 2). ROI analysis of mCherry and PNCP was applied in ESM Suppl. Fig. 2. The results demonstrated that the fluorescence intensity of mCherry was low compared with that of PNCP.

In Vivo Fluorescence Imaging of PNCP in Mice

In order to achieve deep and accurate imaging in BALB/c nude mice, we used real-time and sensitive pCLE which was carried out *in vivo* on the micro level with minor wounds [36].

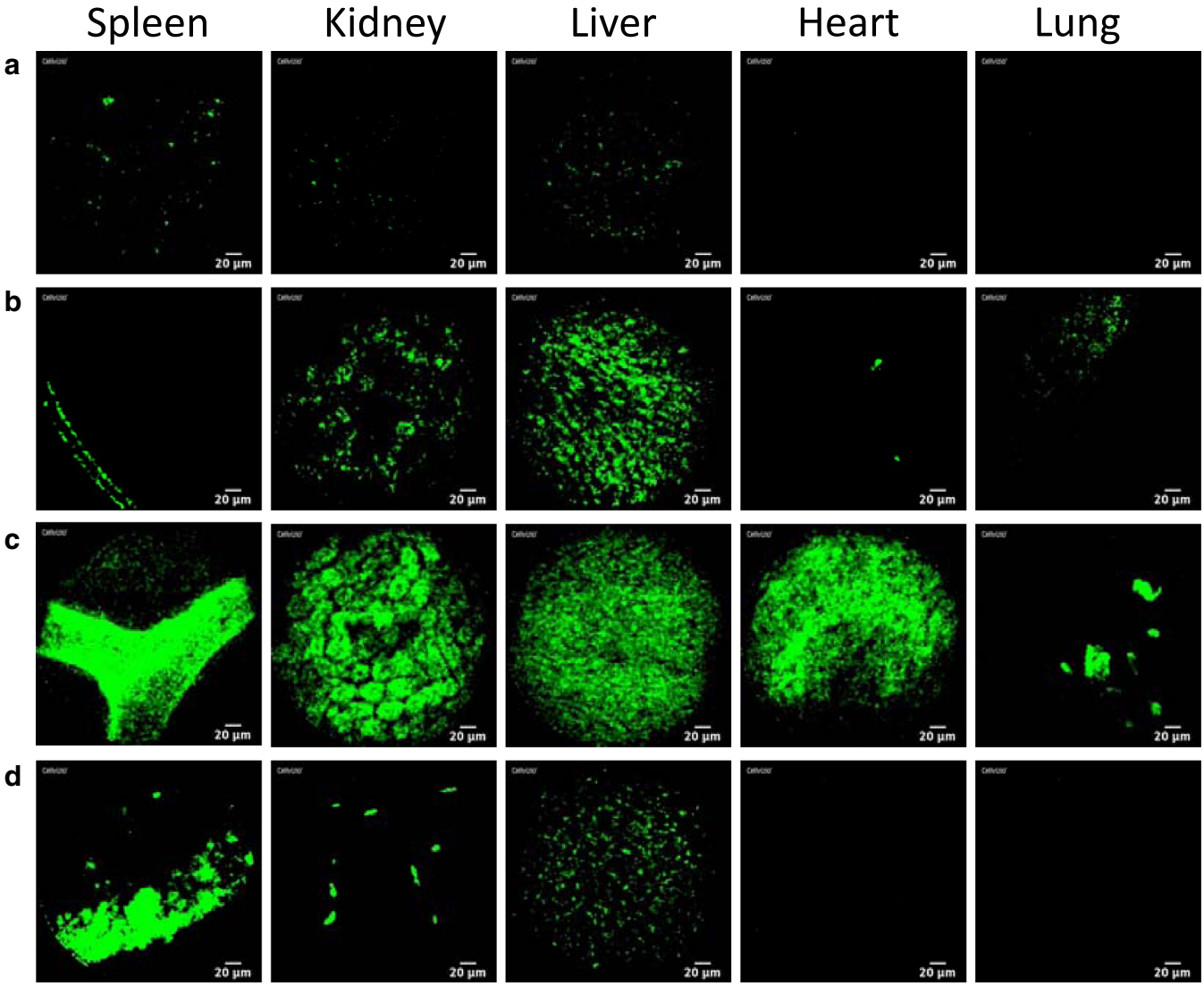

Fig. 3. pCLE imaging organs of mice after i.v. injection of labeled $SKOV_3$-mCherry. The green (PNCP) channel was excited at 488 nm and collected from 505 to 700 nm. **a** Blank control. Observation of organs at **b** 40 min, **c** 6 h, and **d** 30 h post-injection.

In Fig. 3a, only isolated point signals emerged in the spleen, kidney, and liver of blank mice without injection. As shown in Fig. 3b–d, dominate organs were imaged at 40 min, 6 h, and 30 h after i.v. injection, respectively. According to the picture recordings, the dot shape and vessel structure were two main types of signals. Intensity of five organs reached the strongest at 6 h post i.v. injection (Fig. 3c). Compared with other organs, the signal of spleen lasts longer, and clear contour still existed even after 30 h. Furthermore, distinct vasculatures in the spleen at 6 h were exampled in ESM Suppl. Fig. 3. It provided parallel and bifurcated morphologies *in vivo* (ESM Videos 1 and 2). The diameter of vessels ranged from 16 to 69 μm and from 6 to 25 μm in pictures of the spleen and kidney, respectively. To conclude, labeled cells exhibited more accumulation and adhesion to the vessel walls at 6 h than other time points. The critical margin of vessels could be recorded by pCLE.

In Fig. 4a of i.p. injection, the fluorescence still remained bright after 6 days especially in the spleen and heart. Dot-like fluorescence was found to form the vessels in the spleen; meanwhile, signals were distributed in the heart relatively. The perfusion of spots highlight vessels in the spleen at 6 days was detected, and it was consistent as observed in i.v. injection.

Comparatively, in Fig. 4b, c of inguinal lymph node injection, the results displayed the fluorescence dispersed in tissues. It indicated that cells migrated from the injection site to prime organs. With the time going on, cells accumulated in detoxification organs increased. To determine whether cells had selectivity of accumulation in organs at a histological level, we checked the frozen sections of three examples by CLSM in ESM Suppl. Fig. 4. On the basis of histology, the fluorescence of PNCP in the kidney, liver, and heart was intense while the intensity in the spleen and lung was weak.

Discussion

In this study, polymer dot–labeled SKOV3-mCherry cells were syringed into nude mice by intravenous injection, intraperitoneal injection, and inguinal lymph node injection, respectively. Clear vasculatures were displayed in the spleen at 6 h post intravenous injection. Besides, the accumulations of cells were observed in detoxification organs like the spleen and kidney after the inguinal lymph node injection increased with time. In comparison, polymer dot–labeled $SKOV_3$ cells without the expression of mCherry mainly clustered in the lung during different periods post i.v. injection (ESM Suppl. Fig. 5). This result indicated that the expression of mCherry may change the nature of original $SKOV_3$ cells.

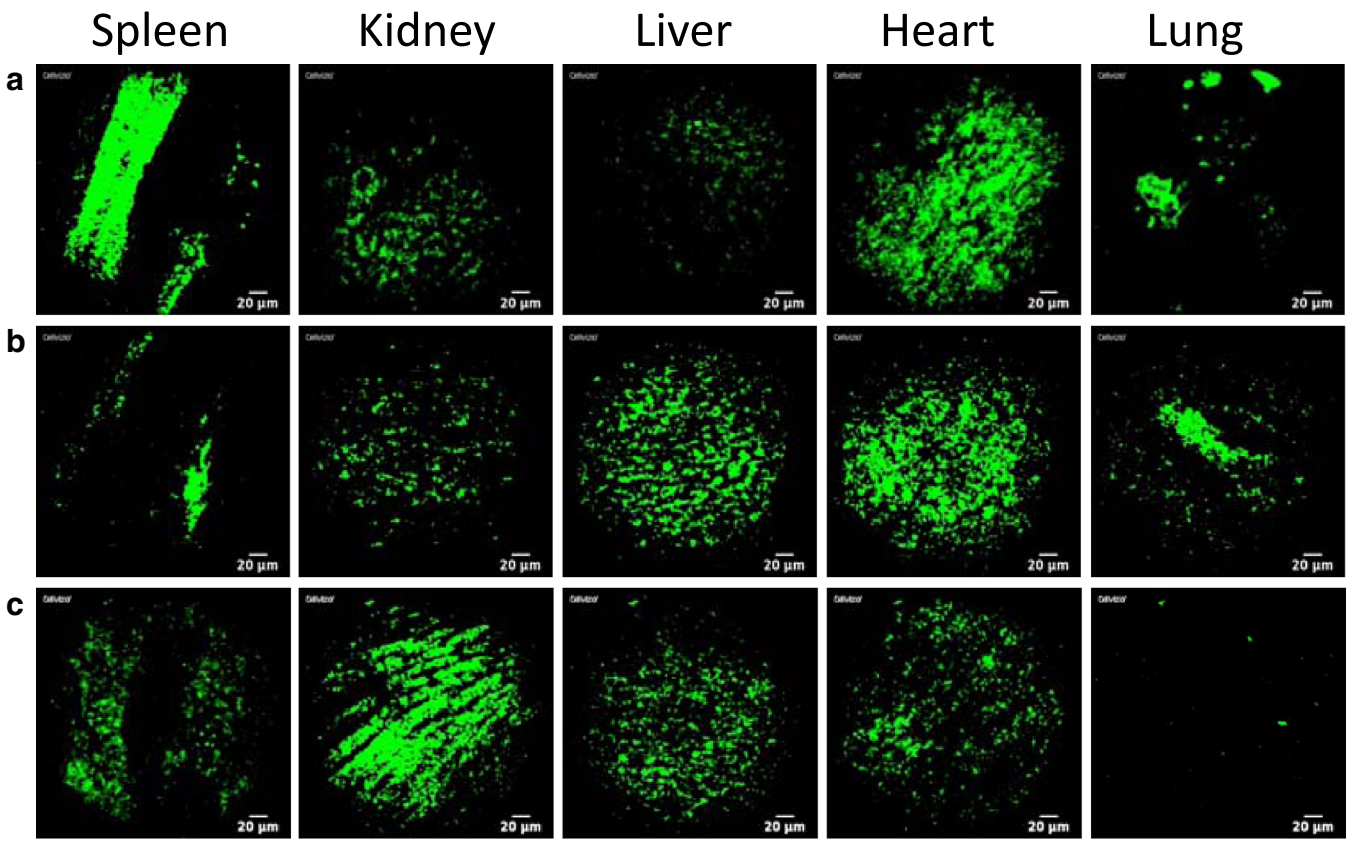

Fig. 4. pCLE imaging organs of mice at **a** 6 days post i.p. injection of labeled $SKOV_3$-mCherry, **b** 8 days, and **c** 15 days post-inguinal lymph node injection of labeled $SKOV_3$-mCherry.

pCLE is rapidly emerged in clinic with minimal invasiveness as a microscopic imaging. It provides high magnification and superior resolution. Compared with fluorescein, fluorescence imaging using polymer dots even lasts for 36 days [21]. pCLE can detect the accumulation sites of cells and observe the flow of vessels instead of 2-deoxy-2-[^{18}F]fluoro-D-glucose ([^{18}F]FDG) PET imaging [37]. We applied an easy and effective method to track $SKOV_3$-mCherry cells circulating in mice *via* different injection sites. It helped study the distribution of cells in organs and implied that pathological changes in organs were connected with the migration of cancer cells. In the future, pCLE can be one of the visualization tools to track cancer cells by means of fluorescence techniques [38].

Conclusion

This study focused on tracking $SKOV_3$-mCherry cells in BALB/c nude mice at a tissue level by combined polymer dots with pCLE. Interestingly, the real-time microscopic imaging displayed the flow of labeled cells in the vessels of organs. The research can establish a promising way for targeting cells. Besides, other imaging modalities like photoacoustic imaging could be combined with pCLE to observe pathological processes of malignant diseases.

Funding. This study was supported by grants from the National Key R&D Program of China (2016YFC1303100), the National Natural Science Foundation of China (81671738, 81301261, and 21374059), the Shanghai Pujiang Project (13PJ1405000), and the Medicine-Engineering Cross Project of Shanghai Jiao Tong University (YG2016MS73).

Compliance with Ethical Standards

Ethical Approval

All animal experiments were performed in accordance with the guidelines of the Institutional Animal Care and Use Committee at Shanghai Jiao Tong University (Shanghai, China).

Conflict of Interest

The authors declare that they have no conflict of interest.

References

1. Chen D, Wu I, Liu Z, Tang Y, Chen H, Yu J, Wu C, Chiu DT (2017) Semiconducting polymer dots with bright narrow-band emission at 800 nm for biological applications. Chem Sci 8:3390–3398
2. Jeong S, Jung Y, Bok S, Ryu YM, Lee S, Kim YE, Song J, Kim M, Kim SY, Ahn GO, Kim S (2018) Multiplexed *in vivo* imaging using size-controlled quantum dots in the second near-infrared window. Adv Healthc Mater. https://doi.org/10.1002/adhm.201800695
3. Geng J, Li K, Ding D, Zhang X, Qin W, Liu J, Tang BZ, Liu B (2012) Lipid-PEG-folate encapsulated nanoparticles with aggregation induced emission characteristics: cellular uptake mechanism and two-photon fluorescence imaging. Small 8:3655–3663
4. Xiong L, Guo Y, Zhang Y, Cao F (2016) Highly luminescent and photostable near-infrared fluorescent polymer dots for long-term tumor cell tracking in vivo. J Mater Chem B 4:202–206
5. Li J, Rao J, Pu K (2018) Recent progress on semiconducting polymer nanoparticles for molecular imaging and cancer phototherapy. Biomaterials 155:217–235
6. Zhen X, Xie C, Pu K (2018) Temperature-correlated afterglow of a semiconducting polymer nanococktail for imaging-guided photothermal therapy. Angew Chem 130:4002–4006
7. Guo L, Ge J, Wang P (2018) Polymer dots as effective phototheranostic agents. Photochem Photobiol 94:916–934
8. Miao Q, Xie C, Zhen X, Lyu Y, Duan H, Liu X, Jokerst JV, Pu K (2017) Molecular afterglow imaging with bright, biodegradable polymer nanoparticles. Nat Biotechnol 35:1102–1110
9. Kim J, Lee TS (2018) Emission tuning with size-controllable polymer dots from a single conjugated polymer. Small 1702758:1–7
10. Jiang Y, Pu K (2018) Molecular fluorescence and photoacoustic imaging in the second near-infrared optical window using organic contrast agents. Adv Biosys 1700262:1–10
11. Guo Y, Li Y, Yang Y, Tang S, Zhang Y, Xiong L (2018) Multiscale imaging of brown adipose tissue in living mice/rats with fluorescent polymer dots. ACS Appl Mater Inter 10:20884–20896
12. Zhu H, Fang Y, Zhen X, Wei N, Gao Y, Luo KQ, Xu C, Duan H, Ding D, Chen P, Pu K (2016) Multilayered semiconducting polymer nanoparticles with enhanced NIR fluorescence for molecular imaging in cells, zebrafish and mice. Chem Sci 7:5118–5125
13. Jiang Y, Pu K (2018) Multimodal biophotonics of semiconducting polymer nanoparticles. Accounts Chem Res 51:1840–1849
14. Ganta S, Singh A, Kulkarni P, Keeler AW, Piroyan A, Sawant RR, Patel NR, Davis B, Ferris C, O'Neal S, Zamboni W, Amiji MM, Coleman TP (2015) EGFR targeted theranostic nanoemulsion for image-guided ovarian cancer therapy. Pharm Res 32:2753–2763
15. Yang Q, Yang Y, Zhou N, Tang K, Lau WB, Lau B, Wang W, Xu L, Yang Z, Huang S, Wang X, Yi T, Zhao X, Wei Y, Wang H, Zhao L, Zhou S (2018) Epigenetics in ovarian cancer: premise, properties, and perspectives. Mol Cancer 17:109
16. Li L, Bi X, Sun H, Liu S, Yu M, Zhang Y, Weng S, Yang L, Bao Y, Wu J, Xu Y, Shen K (2018) Characterization of ovarian cancer cells and tissues by Fourier transform infrared spectroscopy. J Ovarian Res 11:64
17. Viswanathan S, Rani C, Delerue-Matos C (2012) Ultrasensitive detection of ovarian cancer marker using immunoliposomes and gold nanoelectrodes. Anal Chim Acta 726:79–84
18. Giri S, Shah SH, Batra K, Anu-Bajracharya, Jain V, Shukla H, Sekhon R, Rawal S (2016) Presentation and management of inguinal lymphadenopathy in ovarian cancer. Indian J Surg Oncol 7:436–440
19. Zhang B, Chen F, Xu Q et al (2017) Revisiting ovarian cancer microenvironment: a friend or a foe? Protein Cell 9:674–692
20. Pu T, Xiong L, Liu Q, Zhang M, Cai Q, Liu H, Sood AK, Li G, Kang Y, Xu C (2017) Delineation of retroperitoneal metastatic lymph nodes in ovarian cancer with near-infrared fluorescence imaging. Oncol Lett 14:2869–2877
21. Ke C, Fang C, Yan J et al (2017) Molecular engineering and design of semiconducting polymer dots with narrow-band, near-infrared emission for *in vivo* biological imaging. ACS Nano 11:3166–3177
22. Wang KK, Carr-Locke DL, Singh SK, Neumann H, Bertani H, Galmiche JP, Arsenescu RI, Caillol F, Chang KJ, Chaussade S, Coron E, Costamagna G, Dlugosz A, Ian Gan S, Giovannini M, Gress FG, Haluszka O, Ho KY, Kahaleh M, Konda VJ, Prat F, Shah RJ, Sharma P, Slivka A, Wolfsen HC, Zfass A (2015) Use of probe-based confocal laser endomicroscopy (pCLE) in gastrointestinal applications. A consensus report based on clinical evidence. United Eur Gastroenterol J 3:230–254
23. Chene G, Chauvy L, Buenerd A, Moret S, Nadaud B, Beaufils E, le Bail-Carval K, Chabert P, Mellier G, Lamblin G (2017) In vivo confocal laser endomicroscopy during laparoscopy for gynecological surgery: a promising tool. J Gynecol Obstet Hum Reprod 46:565–569
24. Bisschops R, Bergman J (2010) Probe-based confocal laser endomicroscopy: scientific toy or clinical tool? Endoscopy 42:487–489
25. Wallace MB, Fockens P (2009) Probe-based confocal laser endomicroscopy. Gastroenterology 136:1509–1513
26. Richardson C, Colavita P, Dunst C, Bagnato J, Billing P, Birkenhagen K, Buckley F, Buitrago W, Burnette J, Leggett P, McCollister H, Stewart K, Wang T, Zfass A, Severson P (2018) Real-time diagnosis of Barrett's esophagus: a prospective, multicenter study comparing confocal laser endomicroscopy with conventional histology for the identification of intestinal metaplasia in new users. Surg Endosc. https://doi.org/10.1007/s00464-018-6420-9
27. Wu L, Yu H, Zhou R, Luo J, Zhao J, Li Y, Wang K, Wang Y, Li H (2018) Probe-based confocal laser endomicroscopy for diagnosis of

nasopharyngeal carcinoma *in vivo*. Laryngoscope. https://doi.org/10.1002/lary.27450
28. Xiong L (2016) Recent advances on near-infrared-emitting poly[2-methoxy-5-(2-ethylhexyloxy)-1,4-phenylenevinylene] polymer dots for *in vivo* imaging. Gen Chem 2:99–106
29. Cao F, Guo Y, Li Y et al (2018) Fast and accurate imaging of lymph node metastasis with multifunctional near-infrared polymer dots. Adv Funct Mater 1707174:1–18
30. Guo Y, Cao F, Li Y, Xiong L (2017) Facilely synthesized pH-responsive fluorescent polymer dots entrapping doped and coupled doxorubicin for nucleus-targeted chemotherapy. J Mater Chem B 5:2921–2930
31. Xiong L, Cao F, Cao X, Guo Y, Zhang Y, Cai X (2015) Long-term-stable near-infrared polymer dots with ultrasmall size and narrow-band emission for imaging tumor vasculature *in vivo*. Bioconjug Chem 26:817–821
32. Trottmann M, Stepp H, Sroka R, Heide M, Liedl B, Reese S, Becker AJ, Stief CG, Kölle S (2015) Probe-based confocal laser endomicroscopy (pCLE)–a new imaging technique for in situ localization of spermatozoa. J Biophotonics 8:415–421
33. Wu G, Wang Z, Bian X, du X, Wei C (2014) Folate-modified doxorubicin-loaded nanoparticles for tumor-targeted therapy. Pharm Biol 52:978–982
34. Ocak M, Gillman AG, Bresee J, Zhang L, Vlad AM, Müller C, Schibli R, Edwards WB, Anderson CJ, Gach HM (2015) Folate receptor-targeted multimodality imaging of ovarian cancer in a novel syngeneic mouse model. Mol Pharm 12:542–553
35. Cao F, Xiong L (2016) Folic acid functionalized PFBT fluorescent polymer dots for tumor imaging. Chinese J Chem 34:570–575
36. Meining A, Shah RJ, Slivka A, Pleskow D, Chuttani R, Stevens PD, Becker V, Chen YK (2012) Classification of probe-based confocal laser endomicroscopy findings in pancreaticobiliary strictures. Endoscopy 44:251–257
37. Han S, Woo S, Suh CH, Lee JJ (2018) Performance of pre-treatment ^{18}F-fluorodeoxyglucose positron emission tomography/computed tomography for detecting metastasis in ovarian cancer : a systematic review and meta-analysis. J Gynecol Oncol 29
38. Trottmann M, Stepp H, Sroka R, Heide M, Liedl B, Reese S, Becker AJ, Stief CG, Kölle S (2015) Probe-based confocal laser endomicroscopy (pCLE) - a new imaging technique for in situ localization of spermatozoa. J Biophotonics 8:415–421